JOURNAL OF GUIDANCE, CONTROL, AND DYNAMICS
Vol. 30, No. 1, January–February 2007

Effect of Equinoctial Precession on Geosynchronous Earth Satellites

Pini Gurfil*
Technion—Israel Institute of Technology, 32000 Haifa, Israel

DOI: 10.2514/1.21479

The long-periodic effects of the equinoctial precession on geosynchronous Earth orbit satellites are investigated. The equations of motion in a reference frame that coprecesses with the Earth are developed, and the resulting variational equations are derived using mean classical orbital elements. The Earth gravitational model includes the J_2 and J_3 zonal harmonics, which induce the equinoctial precession due to the lunisolar gravitational torque. It is shown that the ever-growing lifetime and mass of geosynchronous Earth orbit satellites render the equinoctial precession a significant factor, which should be taken into account during mission design, as it affects north–south stationkeeping maneuvers. The equilibria of the variational equations including the zonal harmonics and the equinoctial precession are investigated and a class of stable frozen orbits which are equinoctial precession invariant is derived.

Nomenclature

a	=	semimajor axis
e	=	eccentricity
f	=	true anomaly
$\mathcal{H}$	=	Hamiltonian
h	=	angular momentum
$\mathcal{I}$	=	inertial reference frame
i	=	inclination
K_1, K_2	=	constant Hamiltonians
$\mathcal{L}$	=	Lagrangian
M	=	mean anomaly
m	=	mass
n	=	mean motion
P	=	Poisson matrix
$\mathcal{P}$	=	perifocal reference frame
p	=	semilatus rectum
R	=	perturbing potential
R_z	=	gravitational potential
$\mathcal{R}$	=	coprecessing reference frame
R_p	=	precessional perturbing potential
R_z	=	zonal perturbing potential
$\boldsymbol{r}$	=	position vector
$\boldsymbol{u}$	=	precessional angular velocity vector
$\boldsymbol{v}$	=	velocity vector
$\boldsymbol{\alpha}$	=	orbital elements set
$\Delta \boldsymbol{F}$	=	disturbing specific force
$\Delta\mathcal{H}$	=	disturbing Hamiltonian
$\Delta\mathcal{L}$	=	disturbing Lagrangian
η	=	eccentricity measure
μ	=	gravitational constant
$\boldsymbol{\Phi}$	=	gauge function
ϕ	=	colatitude angle
ψ	=	obliquity of the ecliptic
Ω	=	longitude of ascending node
ω	=	argument of perigee
ω_l	=	natural libration frequency
$(\cdot)_0$	=	initial condition
$(\dot{\underline{\cdot}})$	=	time differentiation
$(\bar{\cdot})$	=	mean value
$\|\cdot\|$	=	Euclidean vector norm

Received 30 November 2005; revision received 23 May 2006; accepted for publication 8 June 2006.

*Senior Lecturer, Faculty of Aerospace Engineering; pgurfil@technion.ac.il. Senior Member AIAA.

I. Introduction

GEOSYNCHRONOUS Earth orbit (GEO) satellites constitute a major portion of commercial space missions. With recent progress in orbit design and stationkeeping techniques, fuel consumption is no longer the limiting factor of GEO mission lifetime. Rather, the end of life condition for a growing number of communication satellites is expected to be a breakdown of the power system, stemming from either battery failure or solar array degradation due to radiation effects [1].

This fact has encouraged the development of durable and robust power systems extending the lifetime of GEO satellites. The use of rechargeable lithium-ion batteries, pioneered by the Eutelsat W3A satellite [2], is expected to extend the typical mission lifetime of GEO satellites to 15 years of reliable operation [3]. An additional trend in GEO satellites is an increase of the overall mass, requiring more propellent for orbit raising and stationkeeping.

The considerable lifetime extension of GEO satellites brings into play an orbital perturbation that is insignificant for short mission lifetimes or for low-Earth orbit (LEO) satellites: The equinoctial precession (EP), which is a circular motion of the Earth's spin axis with respect to an inertial frame. It is caused mainly by the lunisolar torque (planetary effects induce precession of the ecliptic; this effect is neglected in the current study) on Earth's equatorial bulge and has a period of approximately 25,770 years [4]. The EP may be viewed as an orbital perturbation due to the fact that the Earth-centered reference frame used for defining the orbital elements is in fact noninertial [5]. The EP thus induces a long-periodic variation of the orbital elements. However, because the period of the EP is much larger than the satellite's lifetime, its effect on the orbital elements may be viewed as secular for all practical purposes. This effect is more significant for long mission lifetimes and high-Earth orbits due to the fact that the EP perturbing potential is proportional to the orbital angular momentum.

A seminal analytical study of the orbital dynamics of a natural satellite about an oblate precessing planet was performed by Goldreich [6], taking into account the J_2 zonal harmonics only and assuming a constant precessional angular velocity. In a later work, a higher-fidelity model for the EP was used to refine Goldreich's results [7]. Recently, it has been shown that the orbital elements used to model the long-periodic effects of the EP are nonosculating, due to the fact that the EP perturbing potential is velocity dependent [8]. This observation will be explained in the sequel.

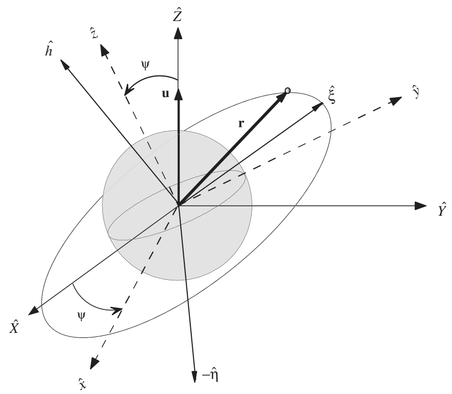

Fig. 1 Inertial, coprecessing and perifocal reference frames.

However, none of the aforementioned works has examined the effect of the EP on artificial Earth satellites. GEO satellites are subjected to a myriad of orbital perturbations, such as solar radiation pressure [9], Earth's oblateness (J_2), tesseral resonance [10], and lunisolar gravitation [11]. This paper shows that the EP should be taken into account when analyzing orbital perturbations of extended-lifetime GEO satellites in addition to the common perturbations. In particular, the EP has a nonnegligible effect on north–south stationkeeping as it induces long-periodic inclination variations.

In the present work, we shall investigate the intercoupling between the zonal gravitational harmonics and EP, while neglecting the nutation of Earth's spin axis. This approach stems from the mechanism generating the EP, which is attributed mostly to the zonal harmonics of the gravitational potential. Hence, zonal perturbations and EP may be regarded as a single realm of orbital perturbations. The main question raised in this work, therefore, may be formulated as follows: Assume that longitudinal perturbations resulting from tesseral harmonics and solar radiation pressure have been corrected by east–west stationkeeping, and long-periodic inclination oscillations have been accounted for by north–south stationkeeping. What is the additional fuel budget required due to the EP?

To answer this question, we start by deriving the potential of the EP perturbing force and expressing it in terms of classical orbital elements. Then we use Lagrange's planetary equations (LPEs) to derive the variational equations of the mean classical orbital elements subjected to zonal perturbations and EP. An illustrative example shows that the EP induces an out-of-plane excursion due to a long-periodic inclination variation, requiring additional north–south stationkeeping maneuvers. Equilibrium solutions of the variational equations are utilized to derive stable frozen orbits, which are invariant under the EP, thus minimizing the propellent mass needed for stationkeeping. A simulation is carried out to verify the analytical observations.

II. Background

In the discussion to follow, we shall use the following reference frames, depicted by Fig. 1:

$\mathcal{I}$, an Earth-centered, inertial, Cartesian, rectangular, dextral (CRD) frame. The fundamental plane is the ecliptic plane, the positive $\hat{X}$ axis is the vernal equinox of fixed epoch, the $\hat{Z}$ axis points in the direction of the celestial north pole, and the $\hat{Y}$ axis completes the setup.

$\mathcal{R}$, a noninertial CRD frame which coprecesses, but does not spin, with the Earth. The fundamental plane is Earth's equatorial plane, the positive $\hat{x}$ axis is the instantaneous vernal equinox, the $\hat{z}$ axis points in the direction of the north pole, and the $\hat{y}$ axis completes the setup.

$\mathcal{P}$, a noninertial perifocal CRD frame. The fundamental plane is the instantaneous orbital plane, the positive $\hat{\xi}$ axis points in the direction of the instantaneous perigee, the $\hat{h}$ axis is normal to the instantaneous orbital plane and points in the direction of the orbital angular momentum, and $\hat{\eta}$ axis completes the setup.

We shall first present the equations of motion for a Keplerian two-body problem and then extend the model to include the effects of EP and zonal harmonics via a variation-of-parameters procedure.

In the Keplerian case, the coordinate system $\mathcal{R}$ is assumed to be an inertial frame. The equations of motion in this frame assuming Newtonian gravitation are given by

$$\ddot{\boldsymbol{r}} + \frac{\mu \boldsymbol{r}}{r^3} = 0 \tag{1}$$

where $\boldsymbol{r} \in \mathbb{R}^3$ is the position vector, and $r = \|\boldsymbol{r}\|$. To solve Eq. (1), it is customary to first express the position vector in the auxiliary perifocal coordinate system, $\mathcal{P}$:

$$\boldsymbol{r}_{\mathcal{P}} = \begin{bmatrix} r\cos f \\ r\sin f \\ 0 \end{bmatrix} \tag{2}$$

where r is given by the usual polar conic equation

$$r = \frac{a(1-e^2)}{1+e\cos f} \tag{3}$$

$f = f(a, e, M_0, t)$ is the true anomaly, and M_0 is the mean anomaly at epoch. The perifocal velocity vector is obtained by writing

$$\dot{\boldsymbol{r}}_{\mathcal{P}} = \dot{f}\left[\frac{\mathrm{d}\boldsymbol{r}}{\mathrm{d}f}\right]_{\mathcal{P}} = \sqrt{\frac{\mu}{a^3(1-e^2)^3}}(1+e\cos f)^2\left[\frac{\mathrm{d}\boldsymbol{r}}{\mathrm{d}f}\right]_{\mathcal{P}} \tag{4}$$

which yields

$$\dot{\boldsymbol{r}}_{\mathcal{P}} = \begin{bmatrix} -\sqrt{\frac{\mu}{a(1-e^2)}}\sin f \\ \sqrt{\frac{\mu}{a(1-e^2)}}(e+\cos f) \\ 0 \end{bmatrix} \tag{5}$$

To solve for $\boldsymbol{r}$ and $\dot{\boldsymbol{r}}$, we need to use a rotation matrix from $\mathcal{R}$ to $\mathcal{P}$, denoted $T_{\mathcal{P}}^{\mathcal{R}}$. A standard transformation is given by [12,13]

$$T_{\mathcal{P}}^{\mathcal{R}}(i,\Omega,\omega) = \begin{bmatrix} c(\Omega)c(\omega) - s(\Omega)s(\omega)c(i) & -c(\Omega)s(\omega) - s(\Omega)c(\omega)c(i) & s(\Omega)s(i) \\ s(\Omega)c(\omega) + c(\Omega)s(\omega)c(i) & -s(\Omega)s(\omega) + c(\Omega)c(\omega)c(i) & -c(\Omega)s(i) \\ s(\omega)s(i) & c(\omega)s(i) & c(i) \end{bmatrix} \tag{6}$$

and the compact notation $c(\cdot) = \cos(\cdot)$, $s(\cdot) = \sin(\cdot)$ is used. Using Eqs. (2) and (6), we obtain the general solution to Eq. (1),

$$\boldsymbol{r} = T_{\mathcal{P}}^{\mathcal{R}}(\Omega,\omega,i)\boldsymbol{r}_{\mathcal{P}}(a,e,M_0,t) = \boldsymbol{f}(a,e,i,\Omega,\omega,M_0,t) \tag{7}$$

where M_0 is the mean anomaly at epoch. Substituting (2), (3), and (6) into (7) and simplifying yields

$$\boldsymbol{r} = \begin{bmatrix} x \\ y \\ z \end{bmatrix} = \frac{a(1-e^2)}{1+e\cos f}\begin{bmatrix} \cos(f+\omega)\cos(\Omega) - \cos(i)\sin(f+\omega)\sin(\Omega) \\ \cos(i)\cos(\Omega)\sin(f+\omega) + \cos(f+\omega)\sin(\Omega) \\ \sin(i)\sin(f+\omega) \end{bmatrix} \tag{8}$$

In a similar fashion, the expression for the velocity is given by

$$\boldsymbol{v} = T_{\mathcal{P}}^{\mathcal{R}}(\Omega, \omega, i)\dot{\boldsymbol{r}}_{\mathcal{P}}(a, e, M_0, t) = \boldsymbol{g}(a, e, i, \Omega, \omega, M_0, t) \tag{9}$$

Thus, the inertial position and velocity depend upon time and the classical orbital elements,

$$\boldsymbol{\alpha} = [a, e, i, \Omega, \omega, M_0]^T \tag{10}$$

The above solutions were obtained for the nominal, undisturbed Keplerian motion. When a disturbing specific force, $\Delta\boldsymbol{F}$, is introduced, Eq. (1) is rewritten as

$$\ddot{\boldsymbol{r}} + \frac{\mu\boldsymbol{r}}{r^3} = \Delta\boldsymbol{F} \tag{11}$$

To solve for the resulting non-Keplerian motion, Euler [14] and Lagrange [15] have developed the variation-of-parameters procedure, a general method for solving nonlinear differential equations. In essence, the method suggests to transform the constants of the unperturbed motion, the classical orbital elements, into functions of time, yielding a modified solution of the form

$$\boldsymbol{r} = \boldsymbol{f}[\boldsymbol{\alpha}(t), t] \tag{12}$$

Taking the time derivative of Eq. (12) yields the relationship

$$\dot{\boldsymbol{r}} = \frac{\partial\boldsymbol{r}}{\partial t} + \boldsymbol{\Phi} = \boldsymbol{g} + \boldsymbol{\Phi} \tag{13}$$

where

$$\boldsymbol{\Phi} = \frac{\partial\boldsymbol{f}}{\partial\boldsymbol{\alpha}}\dot{\boldsymbol{\alpha}} \in \mathbb{R}^3 \tag{14}$$

is termed the gauge function. To obtain the variational differential equations describing the temporal change of the classical orbital elements, Eq. (13) is differentiated and substituted into Eq. (11), giving

$$\frac{\partial\boldsymbol{g}}{\partial\boldsymbol{\alpha}}\dot{\boldsymbol{\alpha}} + \dot{\boldsymbol{\Phi}} = \Delta\boldsymbol{F} \tag{15}$$

Multiplying Eq. (15) by $(\partial\boldsymbol{f}/\partial\boldsymbol{\alpha})^T$ and Eq. (14) by $(\partial\boldsymbol{g}/\partial\boldsymbol{\alpha})^T$ and subtracting yields Gauss's variational equations (GVEs) [16]:

$$\dot{\boldsymbol{\alpha}} = P^T\left[\left(\frac{\partial\boldsymbol{f}}{\partial\boldsymbol{\alpha}}\right)^T(\Delta\boldsymbol{F} - \dot{\boldsymbol{\Phi}}) - \left(\frac{\partial\boldsymbol{g}}{\partial\boldsymbol{\alpha}}\right)^T\boldsymbol{\Phi}\right] \tag{16}$$

where P is the 6×6 skew-symmetric Poisson matrix [12], given by

$$P^T = \begin{bmatrix} 0 & 0 & 0 & 0 & 0 & \frac{2}{na} \\ 0 & 0 & 0 & 0 & -\frac{\sqrt{1-e^2}}{na^2 e} & \frac{1-e^2}{na^2 e} \\ 0 & 0 & 0 & -\frac{1}{na^2\sqrt{1-e^2}\sin i} & \frac{\cot i}{na^2\sqrt{1-e^2}} & 0 \\ 0 & 0 & \frac{1}{na^2\sqrt{1-e^2}\sin i} & 0 & 0 & 0 \\ 0 & \frac{\sqrt{1-e^2}}{na^2 e} & -\frac{\cot i}{na^2\sqrt{1-e^2}} & 0 & 0 & 0 \\ -\frac{2}{na} & -\frac{1-e^2}{na^2 e} & 0 & 0 & 0 & 0 \end{bmatrix} \tag{17}$$

and $n = \sqrt{\mu/a^3}$ is the mean motion.

The variations-of-parameters procedure, which maps from $(\boldsymbol{r}, \dot{\boldsymbol{r}})$ into $(\boldsymbol{\alpha}, \dot{\boldsymbol{\alpha}})$, involves an inherent freedom, permitting one to impose three extra conditions. Lagrange chose to impose the constraint $\boldsymbol{\Phi} = \boldsymbol{0}$, which is also known as the Lagrange or osculation constraint. The Lagrange constraint postulates that the trajectory in the inertial configuration space is always tangential to an "instantaneous" ellipse (or hyperbola) defined by the instantaneous values of the time-varying orbital elements $\boldsymbol{\alpha}(t)$. This instantaneous orbit is called osculating orbit. Accordingly, the orbital elements which satisfy the Lagrange constraint are called osculating orbital elements. The Lagrange constraint, however, is completely arbitrary and may be freely chosen by the user [16–19]. The use of a generalized Lagrange constraint, that is, $\boldsymbol{\Phi} \neq \boldsymbol{0}$, gives rise to nonosculating orbital elements. We shall now show that in the case of velocity-dependent perturbations (such as the EP), selecting $\boldsymbol{\Phi} \neq \boldsymbol{0}$ is necessary to derive the common form of LPEs [8].

Let $R(\boldsymbol{r}, \dot{\boldsymbol{r}})$ be a position- and velocity-dependent perturbing potential generating some perturbing Lagrangian $\Delta\mathcal{L}(\boldsymbol{r}, \dot{\boldsymbol{r}})$. The resulting perturbing force $\Delta\boldsymbol{F}$ may be expressed in terms of $\Delta\mathcal{L}$ by utilizing the Euler–Lagrange equations,

$$\Delta\boldsymbol{F} = \frac{\partial\Delta\mathcal{L}}{\partial\boldsymbol{r}} - \frac{\mathrm{d}}{\mathrm{d}t}\left(\frac{\partial\Delta\mathcal{L}}{\partial\dot{\boldsymbol{r}}}\right) \tag{18}$$

Substituting into (16) yields

$$\dot{\boldsymbol{\alpha}} = P^T\left\{\left(\frac{\partial\boldsymbol{f}}{\partial\boldsymbol{\alpha}}\right)^T\left[\frac{\partial\Delta\mathcal{L}}{\partial\boldsymbol{r}} - \frac{\mathrm{d}}{\mathrm{d}t}\left(\frac{\partial\Delta\mathcal{L}}{\partial\dot{\boldsymbol{r}}} + \boldsymbol{\Phi}\right)\right] - \left(\frac{\partial\boldsymbol{g}}{\partial\boldsymbol{\alpha}}\right)^T\boldsymbol{\Phi}\right\} \tag{19}$$

Choose [20]

$$\boldsymbol{\Phi} = -\frac{\partial\Delta\mathcal{L}}{\partial\dot{\boldsymbol{r}}} \tag{20}$$

and substitute into (19) to get

$$\dot{\boldsymbol{\alpha}} = P^T\left[\left(\frac{\partial\boldsymbol{f}}{\partial\boldsymbol{\alpha}}\right)^T\frac{\partial\Delta\mathcal{L}}{\partial\boldsymbol{r}} + \left(\frac{\partial\boldsymbol{g}}{\partial\boldsymbol{\alpha}}\right)^T\frac{\partial\Delta\mathcal{L}}{\dot{\partial\boldsymbol{r}}}\right] \tag{21}$$

which simplifies via the chain rule [8] and the Legendre transformation [21] into the familiar form (a more elaborate discussion can be found in Appendix A) of LPEs:

$$\dot{\boldsymbol{\alpha}} = P^T\frac{\partial R}{\partial\boldsymbol{\alpha}} \tag{22}$$

Although Eq. (22) assumed the common form of LPEs, the orbital elements $\boldsymbol{\alpha}$ are nonosculating, as they were obtained for $\boldsymbol{\Phi} \neq \boldsymbol{0}$. However, when the perturbation potential depends upon position only (e.g., high-order zonal gravitational harmonics), Eq. (20) reduces to $\boldsymbol{\Phi} = \boldsymbol{0}$, and the resulting planetary equations assume the same form as in (22) with osculating orbital elements. Consequently, the LPEs can be used to model variations of parameters due to velocity-dependent potentials as well.

A common practice in astrodynamics and celestial mechanics is to obtain the secular and long-periodic effects of a perturbing potential by time-scale separation. This procedure, pioneered by Brouwer [17], is carried out by averaging the planetary equations. In essence, the averaging procedure yields expressions for the secular effect of first-order small perturbations on a satellite orbit assuming that the variations of orbital elements during some given time interval is of second order. The resulting orbital elements are called mean orbital elements.

The averaging of a perturbing potential R is carried out as follows [12]:

$$\bar{R} = \langle R\rangle = \frac{1}{2\pi}\int_0^{2\pi} R\,\mathrm{d}M \tag{23}$$

or, alternatively,

$$\bar{R} = \frac{1}{2\pi}\int_0^{2\pi}\frac{n}{h}Rr^2\,\mathrm{d}f \tag{24}$$

where $h = \sqrt{\mu a(1-e^2)}$ is the orbital angular momentum. To perform the averaging procedure, it is assumed that the perturbing potential is first order small, that is,

$$R = \epsilon \tilde{R}, \qquad \epsilon \ll 1 \tag{25}$$

where $\tilde{R}$ is the nondimensional potential. This assumption guarantees that to first order, time-scale separation renders the mean orbital elements unchanged in the interval $f = [0, 2\pi]$. Hence, the averaged differential equations for the mean orbital elements are obtained by the substituting

$$\boldsymbol{\alpha} \mapsto \bar{\boldsymbol{\alpha}}, \qquad \dot{\boldsymbol{\alpha}} \mapsto \dot{\bar{\boldsymbol{\alpha}}} \tag{26}$$

into the planetary equations. We shall focus in the next sections on the secular effects of perturbations stemming from the EP and its coupling to Earth's zonal harmonics.

III. Equations of Motion in a Precessing Frame

Let $\boldsymbol{r} \in \mathbb{R}^3 \backslash \{0\}$ be the position vector of the satellite in $\mathcal{R}$, and $\boldsymbol{u} \in \mathbb{R}^3$ the angular velocity vector of frame $\mathcal{R}$ relative to frame $\mathcal{I}$. The acceleration of the satellite in the coprecessing frame $\mathcal{R}$ is given by the equation of motion in a rotating frame,

$$\ddot{\boldsymbol{r}} + \frac{\mu \boldsymbol{r}}{r^3} = -2\boldsymbol{u} \times \dot{\boldsymbol{r}} - \boldsymbol{u} \times (\boldsymbol{u} \times \boldsymbol{r}) - \dot{\boldsymbol{u}} \times \boldsymbol{r} \tag{27}$$

Comparing to Eq. (11), we see that the perturbing force due to the EP is given by

$$\Delta \boldsymbol{F} = -2\boldsymbol{u} \times \dot{\boldsymbol{r}} - \boldsymbol{u} \times (\boldsymbol{u} \times \boldsymbol{r}) - \dot{\boldsymbol{u}} \times \boldsymbol{r} \tag{28}$$

Based on previous derivations [6], it is shown in Appendix A that the perturbing potential of the precessional force R_p can be written as

$$R_p = u\sqrt{\mu a(1 - e^2)}(\cos i \cos \psi - \sin i \cos \Omega \sin \psi) \tag{29}$$

where ψ is the obliquity of the ecliptic (see Fig. 1), and $u = \|\boldsymbol{u}\|$ is the precessional angular velocity. Expression (29) has been obtained by assuming uniform precession, $u = \text{const}$ and constant obliquity $\psi = \text{const}$. Using (22), the LPEs become

$$\dot{\boldsymbol{\alpha}} = P^T \frac{\partial R_p}{\partial \boldsymbol{\alpha}} = P^T \frac{\partial \bar{R}_p}{\partial \boldsymbol{\alpha}} \tag{30}$$

The last equality in (30) stems from the fact that R_p is time independent, so that $R_p \equiv \bar{R}_p$ and the effect of the uniform EP is long periodic only. The mean orbital elements are therefore identical to the instantaneous orbital elements, $\boldsymbol{\alpha} \equiv \bar{\boldsymbol{\alpha}}$.

Substituting (17) and (29) into (30), we get the variation of orbital elements due to EP:

$$\frac{\mathrm{d}a}{\mathrm{d}t} = 0 \tag{31}$$

$$\frac{\mathrm{d}e}{\mathrm{d}t} = 0 \tag{32}$$

$$\frac{\mathrm{d}i}{\mathrm{d}t} = -u \sin \Omega \sin \psi \tag{33}$$

$$\frac{\mathrm{d}\Omega}{\mathrm{d}t} = -u(\cot i \cos \Omega \sin \psi + \cos \psi) \tag{34}$$

$$\frac{\mathrm{d}\omega}{\mathrm{d}t} = u \frac{\sin \psi \cos \Omega}{\sin i} \tag{35}$$

$$\frac{\mathrm{d}M_0}{\mathrm{d}t} = 0 \tag{36}$$

Examining Eqs. (31–36) shows that the EP does not affect the semimajor axis, the eccentricity, and the mean anomaly at epoch. However, the precession *does* affect the inclination and induces apsidal and nodal rotations. The periodic dynamics of the precession-perturbed inclination will generate out-of-plane excursion which will cause the satellite to drift, on short time scales, from the reference orbit. We shall investigate this phenomenon in the next section while incorporating zonal gravitational perturbations into the analysis.

As previously discussed, the EP is caused by the effect of the lunisolar gravitational torque on the Earth's equatorial bulge. Thus, the perturbing effect of zonal gravitational harmonics must be included in the variational equations of the classical orbital elements. The gravitational potential including zonal harmonics only is given by [12]

$$R_z = -\frac{\mu}{r} \sum_{k=2}^{\infty} J_k \left(\frac{r_{\text{eq}}}{r}\right)^k P_k(\cos \phi) = -\sum_{k=2}^{\infty} R_{J_k} \tag{37}$$

where ϕ is the colatitude angle, satisfying

$$\cos \phi = \sin(\omega + f) \sin i \tag{38}$$

P_k is a Legendre polynomial of the first kind of order k, and r_{eq} is Earth's equatorial radius.

An important question is where to truncate R_g so as to obtain a realistic model of the zonal gravitational perturbations taking into account the effect of the EP. The answer largely depends on the type of the satellite orbit. In low-Earth orbits, the effect of EP is negligible even for long mission lifetimes, as the oblateness term J_2 markedly dominates the variation of orbital elements. In geosynchronous orbits, however, the effect of EP is much more significant, as the gravitational perturbations decay rapidly with altitude while the precessional potential increases moderately with altitude. To quantify this observation, we shall perform an order-of-magnitude analysis by computing the values of the perturbing potential normalized by the nominal gravitational potential,

$$R_g = -\frac{\mu}{r} \tag{39}$$

The zonal coefficients for Earth are given by

$$J_2 = 1082.63 \times 10^{-6} \tag{40}$$

$$J_3 = -2.532153 \times 10^{-6} \tag{41}$$

$$J_4 = -1.6109877 \times 10^{-6} \tag{42}$$

The precession angular velocity calculated assuming a 25,770-year period [4]:

$$u = 7.7314124597 \times 10^{-12} \ \text{rad/s} \tag{43}$$

and the obliquity of the ecliptic is

$$\psi = 23.45 \ \text{deg} \tag{44}$$

For geosynchronous orbits,

$$a = 42,164 \ \text{km}, \qquad e \approx 0 \tag{45}$$

In addition,

$$|\cos \phi| \le 1 \rightarrow |P_k(\cos \phi)| \le 1 \tag{46}$$

$$|\cos i \cos \psi - \sin i \cos \Omega \sin \psi| \le 1 \tag{47}$$

Substituting (40–47) into (29) and (37) yields

$$\mathcal{O}\left(\frac{R_{J_2}}{R_g}\right) = \mathcal{O}\left[J_2 \left(\frac{r_{\text{eq}}}{r}\right)^2\right] \approx 2.452 \times 10^{-5} \tag{48}$$

$$\mathcal{O}\left(\frac{R_{J_3}}{R_g}\right) = \mathcal{O}\left[J_3\left(\frac{r_{\text{eq}}}{r}\right)^3\right] \approx 8.633 \times 10^{-9} \tag{49}$$

$$\mathcal{O}\left(\frac{R_{J_4}}{R_g}\right) = \mathcal{O}\left[J_4\left(\frac{r_{\text{eq}}}{r}\right)^4\right] \approx 8.266 \times 10^{-10} \tag{50}$$

$$\mathcal{O}\left(\frac{R_p}{R_g}\right) = \mathcal{O}\left(ur\sqrt{\frac{a}{\mu}}\right) \approx 1.068 \times 10^{-7} \tag{51}$$

A few observations regarding (48–51) are in order. First and foremost, we see that the normalized perturbation potential due to the EP is only 2 orders of magnitude smaller than the normalized J_2 potential. In fact, the precessional potential is an order of magnitude larger than the J_3 potential and 2 orders of magnitude larger than the J_4 perturbation. We therefore neglect the J_4 effect in the forthcoming analysis and include the J_2 and J_3 terms only:

$$R_z \approx R_{J_2} + R_{J_3} \tag{52}$$

For comparison, the order of magnitude of the normalized lunisolar gravitational potential is $\approx 5 \times 10^{-6}$ [22]. We stress that although the lunisolar perturbing potential is more dominant than the EP, we treat the precession and the zonals as a single, unified, perturbation, assuming that the inclination drift resulting from lunisolar gravity had been corrected by a preceding north–south maneuver. In other words, we focus here on variations of orbital elements due to the EP.

To continue, we use Eqs. (24), (37), and (38), to drive an expression for the mean potential in terms of mean orbital elements:

$$\bar{R}_z = \frac{n^2 J_2 r_{\text{eq}}^2}{4(1-e^2)^{\frac{3}{2}}}(3\cos^2 i - 1) + \frac{3}{8}\frac{n^2 J_3 r_{\text{eq}}^3 e \sin\omega \sin i(5\cos^2 i - 1)}{a(1-e^2)^{\frac{5}{2}}} \tag{53}$$

The resulting LPEs,

$$\dot{\boldsymbol{\alpha}} = P^T \frac{\partial \bar{R}_z}{\partial \boldsymbol{\alpha}} \tag{54}$$

yield variational equations for the truncated zonal potential, given by

$$\frac{\mathrm{d}a}{\mathrm{d}t} = 0 \tag{55}$$

$$\frac{\mathrm{d}e}{\mathrm{d}t} = -\frac{3}{8}J_3\left(\frac{r_{\text{eq}}}{p}\right)^3 n\eta^2 \cos\omega(5\cos^2 i - 1)\sin i \tag{56}$$

$$\frac{\mathrm{d}i}{\mathrm{d}t} = \frac{3}{8}J_3\left(\frac{r_{\text{eq}}}{p}\right)^3 ne\cos\omega(5\cos^2 i - 1)\cos i \tag{57}$$

$$\frac{\mathrm{d}\Omega}{\mathrm{d}t} = -\tfrac{3}{2}J_2\left(\tfrac{r_{\text{eq}}}{p}\right)^2 n\cos i + \tfrac{3}{8}J_3\left(\tfrac{r_{\text{eq}}}{p}\right)^3 ne\sin\omega(15\cos^2 i - 11) \times \cos i \tag{58}$$

$$\frac{\mathrm{d}\omega}{\mathrm{d}t} = \frac{3}{4}J_2\left(\frac{r_{\text{eq}}}{p}\right)^2 n(5\cos^2 i - 1) - \frac{3}{8}J_3\left(\frac{r_{\text{eq}}}{p}\right)^3 n\frac{\sin\omega}{e\sin i}[\sin^2(i) \times (1 - 5\cos^2 i - 35e^2\cos^2 i) + 4e^2] \tag{59}$$

$$\frac{\mathrm{d}M_0}{\mathrm{d}t} = \frac{3}{4}J_2\left(\frac{r_{\text{eq}}}{p}\right)^2 n\eta(3\cos^2 i - 1) + \frac{3}{8}J_3\left(\frac{r_{\text{eq}}}{p}\right)^3 n\eta\frac{(4e^2-1)}{e} \times \sin\omega\sin i(5\cos^2 i - 1) \tag{60}$$

where $p = a(1-e^2)$ is the semilatus rectum and $\eta = \sqrt{1-e^2}$ is the eccentricity measure.

The high-order zonal harmonics J_3 affects the long-periodic dynamics of all orbital elements except a. In addition, the J_3 effect couples the dynamics of the apsidal rotation to the nodal regression and inclination variation, which are uncoupled under a J_2 perturbation only. This coupling decreases for small eccentricities, as is the case for GEO satellites. This fact will be used subsequently for identifying frozen orbits.

In summary, the orbital dynamics of a satellite subject to the EP and the J_2 and J_3 zonals are obtained by writing

$$\dot{\boldsymbol{\alpha}} = P^T \frac{\partial \bar{R}_p}{\partial \boldsymbol{\alpha}} + P^T \frac{\partial \bar{R}_z}{\partial \boldsymbol{\alpha}} \tag{61}$$

which results in the following variational equations:

$$\frac{\mathrm{d}a}{\mathrm{d}t} = 0 \tag{62}$$

$$\frac{\mathrm{d}e}{\mathrm{d}t} = -\frac{3}{8}J_3\left(\frac{r_{\text{eq}}}{p}\right)^3 n\eta^2 \cos\omega(5\cos^2 i - 1)\sin i \tag{63}$$

$$\frac{\mathrm{d}i}{\mathrm{d}t} = \frac{3}{8}J_3\left(\frac{r_{\text{eq}}}{p}\right)^3 ne\cos\omega(5\cos^2 i - 1)\cos i - u\sin\Omega\sin\psi \tag{64}$$

$$\frac{\mathrm{d}\Omega}{\mathrm{d}t} = -\tfrac{3}{2}J_2\left(\tfrac{r_{\text{eq}}}{p}\right)^2 n\cos i + \tfrac{3}{8}J_3\left(\tfrac{r_{\text{eq}}}{p}\right)^3 ne\sin\omega(15\cos^2 i - 11) \times \cos i - u(\cot i\cos\Omega\sin\psi + \cos\psi) \tag{65}$$

$$\frac{\mathrm{d}\omega}{\mathrm{d}t} = \frac{3}{4}J_2\left(\frac{r_{\text{eq}}}{p}\right)^2 n(5\cos^2 i - 1) - \frac{3}{8}J_3\left(\frac{r_{\text{eq}}}{p}\right)^3 n\frac{\sin\omega}{e\sin i}[\sin^2(i) \times (1 - 5\cos^2 i - 35e^2\cos^2 i) + 4e^2] + u\frac{\sin\psi\cos\Omega}{\sin i} \tag{66}$$

$$\frac{\mathrm{d}M_0}{\mathrm{d}t} = \frac{3}{4}J_2\left(\frac{r_{\text{eq}}}{p}\right)^2 n\eta(3\cos^2 i - 1) + \frac{3}{8}J_3\left(\frac{r_{\text{eq}}}{p}\right)^3 n\eta\frac{(4e^2-1)}{e} \times \sin\omega\sin i(5\cos^2 i - 1) \tag{67}$$

In the next section, we shall investigate Eqs. (62–67) and will be particularly interested in the out-of-plane excursion due to the EP.

IV. Motivating Example

We shall start the analysis of Eqs. (62–67) by presenting a motivating example. Consider a GEO satellite with the initial orbital elements

$$e_0 = 0.01, \qquad i_0 = 0.01 \text{ rad}, \qquad \Omega_0 = 3\pi/4 \text{ rad} \qquad \omega_0 = \pi/2 \text{ rad} \tag{68}$$

For these initial conditions and the parameter values (40–44), let us compare the J_2-perturbed, lunisolar gravitation-free orbital dynamics for the following cases:

$$J_3 = u = 0 \tag{69}$$

$$J_3 \neq 0, \qquad u = 0 \tag{70}$$

$$J_3 = 0, \qquad u \neq 0 \tag{71}$$

$$J_3 \neq 0, \qquad u \neq 0 \tag{72}$$

Integration of the equations of motion (62–67) for cases (70–72) was performed using an eighth-order Runge–Kutta algorithm. The results of the simulation assuming a 15-year mission lifetime are depicted by Figs. 2 and 3.

Figure 2 shows the time histories of the differences of the orbital elements e, i, Ω, and ω for cases (70–72) relative to the J_2-only case, (70). Examining the results for Ω and ω, we see that the curves for the various cases are practically indistinguishable. We also note that the J_3 term slightly modifies the eccentricity, reducing it by about 3 ppm within the given lifetime while increasing the inclination by about 0.002 deg.

However, the precession term u is much more significant. Although not affecting the eccentricity, it reduces the inclination by about $0.00134 \text{ rad} = 0.077$ deg, which is 540 times larger than the inclination change caused by J_3. This is not surprising, as Eq. (64) shows that the secular inclination change for $e \approx 0$ is dominated by the precession term. We shall use this fact in the sequel to decouple the effects of EP and J_3 on the orbital element variations.

The secular precession-induced inclination drift will cause a significant out-of-plane excursion due to the relatively large semimajor axis of GEO orbits, 42,164 km. To estimate the out-of-plane deflection, recall from Eq. (8) the expression for the normal component of motion in the precessing frame $\mathcal{R}$,

$$z = \frac{a(1-e^2)}{1+e\cos f}\sin(i)\sin(f+\omega) \tag{73}$$

For GEO orbits, $e \approx 0$ and $\sin i \approx i$, so that the normal deflection relative to the initial orbit, taking the long-term component of the motion only, may be written in terms of mean orbital elements as

$$\Delta z = z - z_0 = a\sin i - a_0 \sin i_0 \approx a(i - i_0) \tag{74}$$

The secular out-of-plane deflection Δz for cases (69–72) is depicted by Fig. 3. Notably, the precessional angular velocity is the most dominant constituent in the induced long-term normal drift of the satellite, causing a 37 km secular out-of-plane excursion after 10 years and a secular out-of-plane deflection of 57 km after 15 years. For the given time interval, Δz grows almost linearly with time at a rate of -3.8 km/year.

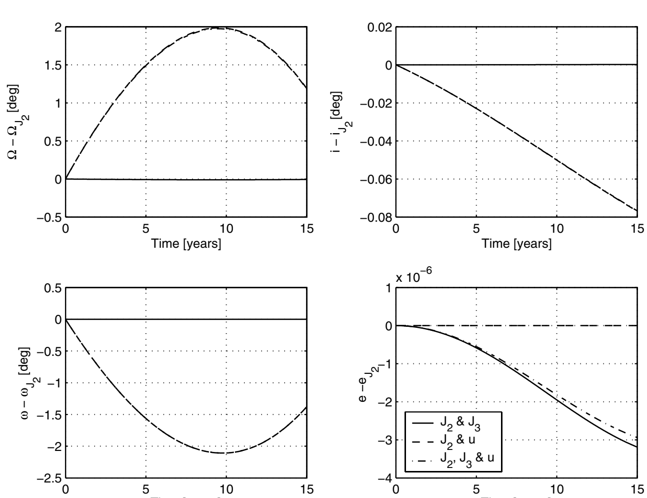

Fig. 2 Examination of the mean orbital elements relative to the J_2-only case shows that the equinoctial precession has a significant secular effect on the inclination.

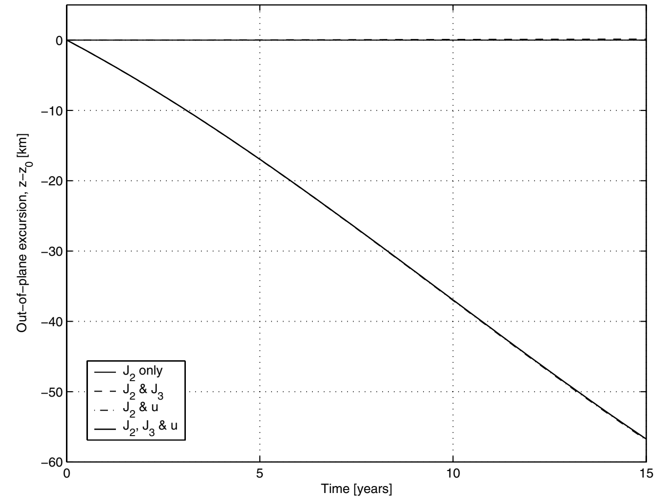

Fig. 3 The secular equinoctial precession-induced inclination variation causes a significant out-of-plane deflection.

The secular inclination variation and resulting out-of-plane deflection require a corrective north–south stationkeeping maneuver. To assess the required velocity correction Δv, we use the GVE [12]

$$\Delta i = \frac{r\cos(f+\omega)}{\sqrt{\mu a(1-e^2)}}\Delta v \tag{75}$$

The minimal GEO velocity correction is therefore

$$\Delta v \approx \sqrt{\frac{\mu}{a}}\Delta i = 4.132 \text{ m/s} \tag{76}$$

Assuming a dimethyl hydrazine propellent with $I_{\text{sp}} = 220$ s and an overall satellite mass of $m_0 = 3000$ kg, the additional fuel mass required for north–south stationkeeping due to the EP can be calculated using the rocket equation:

$$\Delta m = m_0\left[1 - \exp\left(-\frac{\Delta v}{I_{\text{sp}} g_0}\right)\right] = 5.7 \text{ kg} \tag{77}$$

Thus, a nonnegligible amount of additional propellent is required to cancel the secular inclination growth due to the EP. This important observation motivates the forthcoming discussion, dealing with finding orbits that are insusceptible to the effect of EP, eliminating the need for precession-induced north–south storekeeping.

V. Motion About Local Equilibria: Frozen Orbits

Equilibria or partial equilibria of the orbital dynamics in the mean orbital elements phase space are usually referred to as "frozen orbits." Frozen orbits can be found under a myriad of orbital perturbations [23,24]. In the present paper, we shall use the term frozen orbits to denote partial equilibria of the system under the combined effect of J_2, J_3, and the EP. We shall show that the EP modifies the previously found frozen orbits assuming J_2 and J_3 perturbations only [23]. In particular, we shall seek frozen orbits minimizing the EP-induced out-of-plane deflection. To that end, we shall define a nominal dynamic system comprising the J_2 and EP effects, and a perturbed dynamic system that entails the J_3 effect as a disturbance, coupling the dynamics of the line of apsides to the inclination variation and nodal regression. This approach stems from the fact that the J_3 effect is an order of magnitude smaller than the EP for a representing GEO, as shown in the previous section. Consequently, the nominal system under investigation is therefore defined as

$$\dot{\boldsymbol{\alpha}} = P^T\left(\frac{\partial \bar{R}_p}{\partial \boldsymbol{\alpha}} + \frac{\partial \bar{R}_{J_2}}{\partial \boldsymbol{\alpha}}\right) \tag{78}$$

Because of the fact that the averaged precessional and zonal potentials are time invariant, the Hamiltonian (total energy) of (78) constitutes a constant of the motion, denoted by K_1,

$$\bar{R}_p + \bar{R}_{J_2} = K_1 \tag{79}$$

We are interested in the stationary points of system (78) satisfying

$$\frac{\mathrm{d}\Omega}{\mathrm{d}t} = 0, \qquad \frac{\mathrm{d}i}{\mathrm{d}t} = 0 \tag{80}$$

In the nominal system (78), the apsidal dynamics are decoupled from the nodal regression and inclination variation, viz.

$$\frac{\mathrm{d}i}{\mathrm{d}t} = -u \sin\Omega \sin\psi \tag{81}$$

$$\frac{\mathrm{d}\Omega}{\mathrm{d}t} = -\frac{3}{2} J_2 \left(\frac{r_{\mathrm{eq}}}{p}\right)^2 n \cos i - u(\cot i \cos\Omega \sin\psi + \cos\psi) \tag{82}$$

Equations (81) and (82) can be solved in closed form. This procedure is carried out in Appendix B. We shall focus here on the investigation of the dynamics in the vicinity of the equilibria of (81) and (82), which are found by solving the algebraic equations

$$u \sin\Omega_0 \sin\psi = 0 \tag{83}$$

$$\frac{3}{2} J_2 \left(\frac{r_{\mathrm{eq}}}{p}\right)^2 n \cos i_0 + u(\cot i_0 \cos\Omega_0 \sin\psi + \cos\psi) = 0 \tag{84}$$

for Ω_0 and i_0. Denoting

$$c_1 = \frac{3}{2} J_2 \left(\frac{r_{\mathrm{eq}}}{p}\right)^2 n \tag{85}$$

the solutions of (83) and (84) are given by

$$\Omega_0 = 0 \tag{86}$$

$$c_1^2 \sin^4 i_0 + 2c_1 u \sin\psi \sin^3 i_0 + (u^2 - c_1^2)\sin^2 i_0 - 2c_1 u \sin\psi \sin i_0 - u^2 \sin^2\psi = 0 \tag{87}$$

and

$$\Omega_0 = \pi \tag{88}$$

$$c_1^2 \sin^4 i_0 - 2c_1 u \sin\psi \sin^3 i_0 + (u^2 - c_1^2)\sin^2 i_0 + 2c_1 u \sin\psi \sin i_0 - u^2 \sin^2\psi = 0 \tag{89}$$

Explicit expressions for the frozen inclination are straightforwardly found by solving the quartic polynomials (87) and (89) for $\sin i_0$. Once Ω_0 and i_0 are found, a solution for the argument of perigee can be derived by direct integration of (66) with $J_3 = 0$ and the initial condition $\omega(t_0) = \omega_0$:

$$\omega(t) = \left[\frac{3}{4} J_2 \left(\frac{r_{\mathrm{eq}}}{p}\right)^2 n(5\cos^2 i_0 - 1) + u \frac{\sin\psi \cos\Omega_0}{\sin i}\right] t + \omega_0$$

We can now estimate the influence of the J_3 effect on the equilibria (86–89) by considering the perturbed system

$$\dot{\boldsymbol{\alpha}} = P^T \left(\frac{\partial \bar{R}_p}{\partial \boldsymbol{\alpha}} + \frac{\partial \bar{R}_{J_2}}{\partial \boldsymbol{\alpha}} + \frac{\partial \bar{R}_{J_3}}{\partial \boldsymbol{\alpha}}\right) \tag{90}$$

and the constant Hamiltonian

$$\bar{R}_p + \bar{R}_{J_2} + \bar{R}_{J_3} = K_2 \tag{91}$$

Equation (63) shows that the eccentricity variation due to J_3 is of order $\mathcal{O}[J_3(r_{\mathrm{eq}}/p)^3] \approx \mathcal{O}(10^{-8})$, and will therefore be neglected in the analysis (but not in the simulations, which will be carried out using high-fidelity models), that is, we shall assume that

$$e \approx \text{const} = 0 \tag{92}$$

The last equality in (92) stems from the fact that the eccentricity is usually very small (but not zero) in a common GEO.

The next step is to solve Eq. (66) without the simplifying assumption $J_3 = 0$. To that end, rewrite (66) as

$$\frac{\mathrm{d}\omega}{k_1(i_0, \Omega_0) + k_2(i_0, \Omega_0)\sin\omega} = \mathrm{d}t \tag{93}$$

where Ω_0 and i_0 are the equilibria of the nominal system given by (86–89), and k_1, k_2 are defined by

$$k_1(i_0, \Omega_0) = \frac{3}{4} J_2 \left(\frac{r_{\mathrm{eq}}}{p}\right)^2 n(5\cos^2 i_0 - 1) + u \frac{\sin\psi \cos\Omega_0}{\sin i_0} \tag{94}$$

$$k_2(i_0, \Omega_0) = -\frac{3}{8} J_3 \left(\frac{r_{\mathrm{eq}}}{p}\right)^3 n \frac{\sin\omega}{e \sin i_0} [\sin^2 i_0 (1 - 5\cos^2 i - 35e^2 \cos^2 i_0) + 4e^2] \tag{95}$$

Equation (93) is a separable differential equation which can be readily solved by quadrature,

$$\int_{\omega_0}^{\omega} \frac{\mathrm{d}\omega}{k_1 + k_2 \sin\omega} = t - t_0 \tag{96}$$

where

$$\int_{\omega_0}^{\omega} \frac{\mathrm{d}\omega}{k_1 + k_2 \sin\omega} = \begin{cases} \dfrac{2}{\sqrt{k_1^2 - k_2^2}} \tan^{-1} \dfrac{k_1 \tan\frac{\omega}{2} + k_2}{\sqrt{k_1^2 - k_2^2}} \Bigg|_{\omega_0}^{\omega} & \text{for } |k_1| > |k_2| \\ \dfrac{1}{\sqrt{k_2^2 - k_1^2}} \ell n \left(\dfrac{k_1 \tan\frac{\omega}{2} + k_2 - \sqrt{k_2^2 - k_1^2}}{k_1 \tan\frac{\omega}{2} + k_2 + \sqrt{k_2^2 - k_1^2}}\right) \Bigg|_{\omega_0}^{\omega} & \text{for } |k_2| > |k_1| \end{cases} \tag{97}$$

Letting $|k_1| > |k_2|$ and $t_0 = 0$ we arrive at

$$\omega(t) = -2\tan^{-1} \frac{k_2 - \sqrt{k_1^2 - k_2^2} \tan\left[\frac{t\sqrt{k_1^2 - k_2^2}}{2} + \tan^{-1}\left(\frac{k_1 \tan\frac{\omega_0}{2} + k2}{\sqrt{k_1^2 - k_2^2}}\right)\right]}{k_1} \tag{98}$$

We must still account for the J_3-induced intercoupling between the inclination, node, and argument of perigee dynamics. This can be done by a judicious selection of the initial condition ω_0. The equilibrium equations at epoch are

$$\frac{3}{8} J_3 \left(\frac{r_{\mathrm{eq}}}{p}\right)^3 n e \cos\omega_0 (5\cos^2 i_0 - 1)\cos i_0 - u \sin\Omega_0 \sin\psi = 0 \tag{99}$$

$$-\frac{3}{2} J_2 \left(\frac{r_{\mathrm{eq}}}{p}\right)^2 n \cos i_0 + \frac{3}{8} J_3 \left(\frac{r_{\mathrm{eq}}}{p}\right)^3 n e \sin\omega_0 (15\cos^2 i - 11)\cos i_0 - u(\cot i_0 \cos\Omega_0 \sin\psi + \cos\psi) = 0 \tag{100}$$

$$\frac{3}{4} J_2 \left(\frac{r_{\mathrm{eq}}}{p}\right)^2 n(5\cos^2 i_0 - 1) - \frac{3}{8} J_3 \left(\frac{r_{\mathrm{eq}}}{p}\right)^3 n \frac{\sin\omega_0}{e \sin i_0} [\sin^2(i_0) \times (1 - 5\cos^2 i_0 - 35e^2 \cos^2 i_0) + 4e^2] + u \frac{\sin\psi \cos\Omega_0}{\sin i_0} = 0 \tag{101}$$

Letting $\Omega_0 =$ or $\Omega_0 = \pi$ [cf. Eqs. (86) and (88)], the required initial argument of perigee is

$$\omega_0 = \frac{\pi}{2} \quad \text{or} \quad \frac{3\pi}{2} \tag{102}$$

The dynamics of the J_3-perturbed system will be affected by the local stability of the nominal frozen orbits, determined by the eigenvalues of the Jacobian

$$J = \begin{bmatrix} \frac{\partial}{\partial i}\frac{di}{dt} & \frac{\partial}{\partial \Omega}\frac{di}{dt} \\ \frac{\partial}{\partial i}\frac{d\Omega}{dt} & \frac{\partial}{\partial \Omega}\frac{d\Omega}{dt} \end{bmatrix}\Bigg|_{\Omega_0, i_0} = \begin{bmatrix} 0 & -u\cos\Omega_0 \sin\psi \\ c_1 \sin i_0 + u(1+\cot^2 i_0)\cos\Omega_0 \sin\psi & u\sin\Omega_0 \sin\psi \cot i_0 \end{bmatrix} \tag{103}$$

Substituting $\Omega_0 = 0$ [cf. Eq. (86)] into (103) yields

$$J(\Omega_0 = 0) = \begin{bmatrix} 0 & -u\sin\psi \\ c_1 \sin i_0 + u(1+\cot^2 i_0)\sin\psi & 0 \end{bmatrix} \tag{104}$$

which possesses the purely imaginary conjugate eigenvalue pair

$$\lambda_{1,2}[J(\Omega_0 = 0)] = \pm\frac{j}{2}\frac{\sqrt{|6u\sin\psi J_2 r_{\text{eq}}^2 n \sin^3 i_0 + 4p^2u^2\sin^2\psi|}}{p\sin i_0} \tag{105}$$

Similarly, for $\Omega_0 = \pi$ [cf. Eq. (88)],

$$J(\Omega_0 = \pi) = \begin{bmatrix} 0 & u\sin\psi \\ c_1 \sin i_0 - u(1+\cot^2 i_0)\sin\psi & 0 \end{bmatrix} \tag{106}$$

and the eigenvalues are

$$\lambda_{1,2}[J(\Omega_0 = \pi)] = \pm\frac{j}{2}\frac{\sqrt{|6u\sin\psi J_2 r_{\text{eq}}^2 n \sin^3 i_0 - 4p^2u^2\sin^2\psi|}}{p\sin i_0} \tag{107}$$

Hence, the nominal frozen orbits defined by the equilibria (86–89) are locally stable based on the center manifold theorem [25]. A useful approximation for the eigenvalues may be obtained by using the fact that for most GEO satellites $i_0 \approx 0$, and hence $6u\sin\psi J_2 r_{\text{eq}}^2 n\sin^3 i_0 \ll 4p^2u^2\sin^2\psi$, giving

$$\lambda_{1,2}[J(i_0 \approx 0, \Omega_0 = 0)] = \lambda_{1,2}[J(i_0 \approx 0, \Omega_0 = \pi)] \approx \pm j\frac{u\sin\psi}{\sin i_0} = \pm j\omega_l \tag{108}$$

The J_3 input will therefore induce a libration of natural frequency ω_l about the equilibrium state. We shall quantify these observations in the next section.

VI. Frozen Orbit Simulation

Consider a GEO satellite with

$$a = 42,164 \text{ km}, \qquad e = 0.01 \tag{109}$$

so that

$$c_1 = 2.66272736 \times 10^{-9} \text{ rad/s} \tag{110}$$

As shown in the previous section, we must choose either $\Omega_0 = 0$ or $\Omega_0 = \pi$ and $\omega_0 = \pi/2$ or $\Omega_0 = 3\pi/2$ to obtain frozen orbits. In this example, we shall use the initial conditions

$$\Omega_0 = \pi, \qquad \omega_0 = \frac{\pi}{2} \tag{111}$$

Using (110) and (111), the value of the precessional angular velocity (43) and the obliquity of the ecliptic (44), the frozen inclination can be found by solving (89) and taking the solution satisfying $i_0 \in [0, \pi/2]$. The only feasible solution is found to be

$$i_0 = 0.0011524 \text{ rad} = 0.06602776 \text{ deg} \tag{112}$$

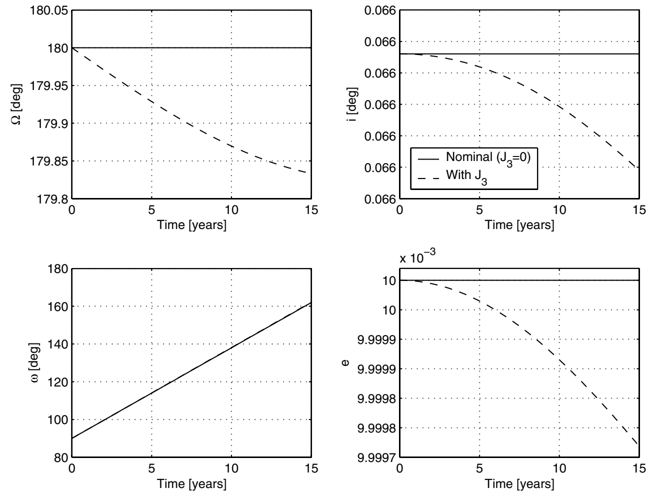

Fig. 4 The mean inclination, longitude of ascending node, and eccentricity remain constant for a frozen orbit and change only slightly under J_3.

which lies well within the geosynchronous window of 0.1×0.1 deg [the frozen inclination found in (112) varies slightly for eccentricities in the range $10^{-5} \leq e_0 \leq 0.01$].

A comparison of the mean orbital elements of the resulting frozen orbit for the cases $J_3 = 0, J_3 \neq 0$ is depicted in Fig. 4. In the nominal case, Ω and i remain constant and equal to the initial values. When J_3 is introduced in to the dynamics, a very slow libration about the nominal equilibria evolves. The frequency of this libration, using Eq. (105), is

$$\omega_l = 2.669818456 \times 10^{-9} \text{ rad/s} \approx c_1 \tag{113}$$

and the period is

$$T_l = 74.6262 \text{ yr} \tag{114}$$

Hence, the drift from the frozen conditions due to J_3 is very slow and is practically insignificant for the lifetimes of GEO satellites, as shown in Fig. 4. This figure shows that during a 15-year mission, Ω_0 decreases by 0.17 deg, i_0 decreases by 3.7×10^{-7} deg, and the frozen eccentricity by 0.28 ppm. The nullification of the inclination drift will eliminate the out-of-plane excursion, which may become significant for the nonfrozen conditions. This fact is illustrated by Fig. 5, comparing Δz for the cases $J_3 = 0$ and $J_3 \neq 0$. For the nominal frozen orbit, including the J_2 and EP only, $\Delta z = 0$. When J_3 is introduced into the simulation, the maximum out-of-plane excursion reaches only 27.4 cm, which is considerably less than the 57 km excursion generated by the nonfrozen conditions (see Sec. IV, Motivating Example). Thus, we have managed to find a frozen orbit which is practically insusceptible to the EP, thus eliminating the need for extra north–south stationkeeping.

The dynamics about the frozen orbits can be established by plotting the equipotential contours of the Hamiltonian K_1. Figure 6 shows the three-dimensional contour plots of K_1 for the parameter values (111) and (112). The stable libration regions about the nominal equilibrium are clearly seen.

VII. Conclusions

The main conclusion from this work is that the equinoctial precession has a nonnegligible effect on geosynchronous Earth orbit satellites characterized by mission lifetimes longer than 10 years, because the normalized perturbation potential due to the EP is only 2 orders of magnitude smaller than the normalized J_2 potential. The

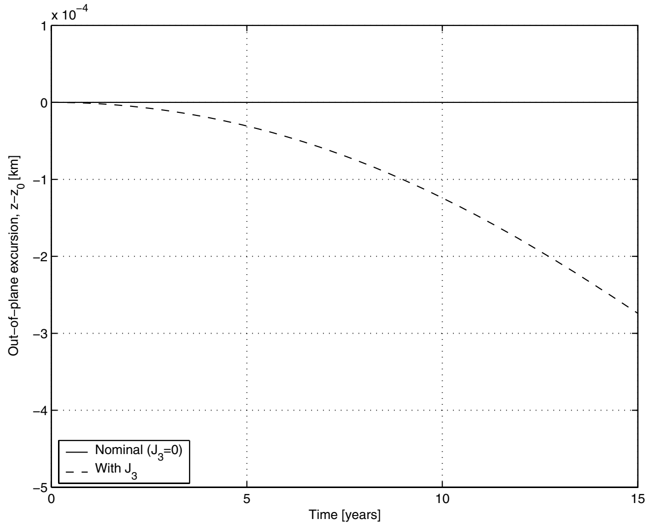

Fig. 5 The frozen orbit practically nullifies the out-of-plane excursion due to the equinoctial precession.

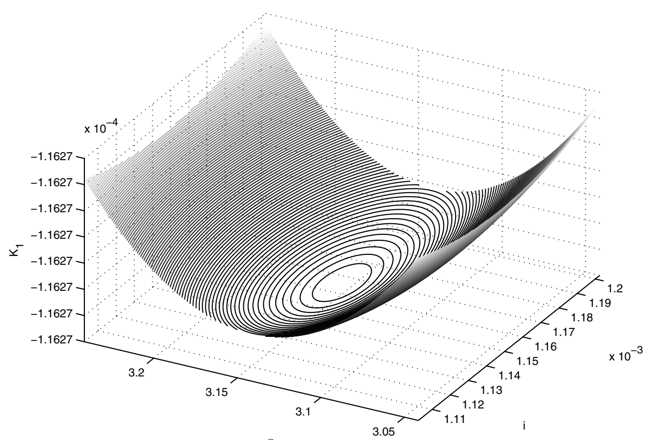

Fig. 6 Three-dimensional contour plot of the nominal Hamiltonian showing the equipotential curves about the equilibrium (frozen orbit).

significance of the EP stems from the fact that the perturbation potential thereof increases with orbital altitude. The secular inclination growth due to the EP requires additional propellent for north–south stationkeeping maneuvers.

We also conclude that there exist frozen orbits that are invariant to the EP assuming a gravitational model comprising zonal harmonics only. These frozen orbits are stable, significantly reducing the EP-induced secular out-of-plane drift and therefore reducing satellite propellent mass. These frozen orbits exist within the geosynchronous window and hence can be used for actual missions.

Appendix A: Equinoctial Precession Perturbing Potential

To derive the position- and velocity-dependent potential of $\Delta \boldsymbol{F}$, we denote by $\mathcal{L}(\boldsymbol{r}, \dot{\boldsymbol{r}})$ the unit-mass Lagrangian of the dynamics in frame $\mathcal{P}$,

$$\mathcal{L}(\boldsymbol{r}, \dot{\boldsymbol{r}}) = \mathcal{L}_0 + \Delta\mathcal{L} \tag{A1}$$

where $\mathcal{L}_0$ is the nominal Lagrangian,

$$\mathcal{L}_0 = \frac{\dot{\boldsymbol{r}} \cdot \dot{\boldsymbol{r}}}{2} + U(\boldsymbol{r}) \tag{A2}$$

$U(\boldsymbol{r})$ is the gravitational potential and $\Delta\mathcal{L}$ is the perturbing Lagrangian due to the equinoctial precession. We next write the Euler–Lagrange equations for a generalized force,

$$\frac{\partial \Delta\mathcal{L}}{\partial \boldsymbol{r}} - \frac{\mathrm{d}}{\mathrm{d}t}\left(\frac{\partial \Delta\mathcal{L}}{\partial \dot{\boldsymbol{r}}}\right) = \Delta \boldsymbol{F} \tag{A3}$$

and verify by direct substitution that the following perturbing Lagrangian satisfies Eq. (A3) [6,8]:

$$\Delta\mathcal{L} = (\dot{\boldsymbol{r}} + \tfrac{1}{2}\boldsymbol{u} \times \boldsymbol{r}) \cdot (\boldsymbol{u} \times \boldsymbol{r}) \tag{A4}$$

The conjugate momenta are, by definition,

$$\boldsymbol{p} \triangleq \frac{\partial \mathcal{L}}{\partial \dot{\boldsymbol{r}}} = \dot{\boldsymbol{r}} + \frac{\partial \Delta\mathcal{L}}{\partial \dot{\boldsymbol{r}}} = \frac{\partial \boldsymbol{r}}{\partial t} + \boldsymbol{\Phi} + \frac{\partial \Delta\mathcal{L}}{\partial \dot{\boldsymbol{r}}} \tag{A5}$$

Using the Legendre transformation, the Hamiltonian is readily calculated by taking

$$\mathcal{H} = \boldsymbol{p}\dot{\boldsymbol{r}} - \mathcal{L} \tag{A6}$$

To obtain the Hamiltonian as a function of the generalized momenta and coordinates only, we substitute the expression for $\dot{\boldsymbol{r}}$ from Eq. (A5) and the Lagrangian from Eq. (A1) into Eq. (A6), yielding

$$\mathcal{H}(\boldsymbol{r}, \boldsymbol{p}) = \boldsymbol{p}\left(\boldsymbol{p} - \frac{\partial \Delta\mathcal{L}}{\partial \dot{\boldsymbol{r}}}\right) - \frac{1}{2}\left(\boldsymbol{p} - \frac{\partial \Delta\mathcal{L}}{\partial \dot{\boldsymbol{r}}}\right)^2 + U(\boldsymbol{r}) - \Delta\mathcal{L} = \frac{\boldsymbol{p}2}{2} - \frac{1}{2}\left(\frac{\partial \mathcal{L}}{\partial \dot{\boldsymbol{r}}}\right)^2 + U(\boldsymbol{r}) - \Delta\mathcal{L} = \frac{\boldsymbol{p}2}{2} + U(\boldsymbol{r}) + \Delta\mathcal{H} \tag{A7}$$

where

$$\Delta\mathcal{H} = -\frac{1}{2}\left(\frac{\partial \Delta\mathcal{L}}{\partial \dot{\boldsymbol{r}}}\right)^2 - \Delta\mathcal{L} = -(\boldsymbol{u} \times \boldsymbol{r}) \cdot \boldsymbol{p} = -\boldsymbol{u} \cdot (\boldsymbol{r} \times \boldsymbol{p}) \tag{A8}$$

Using Eq. (13), we see that choosing

$$\boldsymbol{\Phi} = -\boldsymbol{u} \times \boldsymbol{r} \tag{A9}$$

yields

$$\boldsymbol{p} = \boldsymbol{g} \tag{A10}$$

so that the last expression in (A8) simplifies into

$$\Delta\mathcal{H} = -\boldsymbol{h} \cdot \boldsymbol{u} \tag{A11}$$

where $\boldsymbol{h}$ is the orbital angular momentum,

$$\boldsymbol{h} = \sqrt{\mu a(1 - e^2)}\hat{h} \tag{A12}$$

The perturbing potential satisfies

$$R_p = -\Delta\mathcal{H} = \sqrt{\mu a(1 - e^2)}\hat{h} \cdot \boldsymbol{u} = \sqrt{\mu a(1 - e^2)}\hat{h} \cdot u\hat{Z} \tag{A13}$$

To express the perturbing potential in rotating coordinates, we assume that the obliquity of the ecliptic ψ is constant (i.e., neglect nutational motion) and that the precession is uniform. The transformation from $\mathcal{R}$ to $\mathcal{I}$ is given by

$$\begin{bmatrix} \hat{X} \\ \hat{Y} \\ \hat{Z} \end{bmatrix} = \begin{bmatrix} 1 & 0 & 0 \\ 0 & \cos(\psi) & -\sin(\psi) \\ 0 & \sin(\psi) & \cos(\psi) \end{bmatrix} \begin{bmatrix} \hat{x} \\ \hat{y} \\ \hat{z} \end{bmatrix} \tag{A14}$$

Substituting $\hat{Z}$ from Eq. (A14) into Eq. (A13) yields

$$R_p = \sqrt{\mu a(1 - e^2)}u(\sin\psi\hat{y} + \cos\psi\hat{z})\hat{h} \tag{A15}$$

Using (6), we note that

$$\begin{bmatrix} \hat{\xi} \\ \hat{\eta} \\ \hat{h} \end{bmatrix} = \left(T_{\mathcal{P}}^{\mathcal{R}}\right)^T \begin{bmatrix} \hat{x} \\ \hat{y} \\ \hat{z} \end{bmatrix} \tag{A16}$$

so we can express $\hat{h}$ as

$$\hat{h} = \sin i \sin \Omega \hat{x} - \sin i \cos \Omega \hat{y} + \cos i \hat{z} \tag{A17}$$

resulting in

$$R_p = u\sqrt{\mu a(1-e^2)}(\cos i \cos \psi - \sin i \cos \Omega \sin \psi) \tag{A18}$$

which agrees with the expression obtained by Goldreich [6].

Appendix B: Closed-Form Solutions for the $\Omega - i$ Dynamics

In this Appendix, we shall derive closed-form solutions for Eqs. (81) and (82). To that end, define the transformation

$$q_1 = \sin i \cos \Omega \tag{B1}$$

$$q_2 = \sin i \sin \Omega \tag{B2}$$

Differentiating (B1) and (B2) yields the differential system

$$\begin{aligned} \frac{dq_1}{dt} &= \frac{di}{dt}\cos i \cos \Omega - \frac{d\Omega}{dt}\sin i \sin \Omega \\ \frac{dq_2}{dt} &= \frac{di}{dt}\cos i \sin \Omega + \frac{d\Omega}{dt}\sin i \cos \Omega \end{aligned} \tag{B3}$$

Substituting from (81) and (82), and collecting terms transforms (B3) into

$$\begin{aligned} \frac{dq_1}{dt} &= q_2(c_1 \cos i + u \cos \psi) \\ \frac{dq_2}{dt} &= q_1(u \cos \psi - c_1 \cos i) - u \sin \psi \cos i \end{aligned} \tag{B4}$$

where c_1 is given by (85). For GEO satellites, it holds that $c_1 \cos i \gg u \cos \psi$, so we may use the approximation

$$\frac{dq_1}{dt} \approx q_2 c_1 \cos i \qquad \frac{dq_2}{dt} \approx -(q_1 c_1 + u \sin \psi)\cos i \tag{B5}$$

We shall now transform the independent variable from t to s using the transformation

$$d\,s = c_1 \cos i \, dt \tag{B6}$$

Substituting into (B5) renders the system of linear equations

$$\frac{dq_1}{ds} = q_2 \qquad \frac{dq_2}{ds} = -q_1 - \frac{u}{c_1}\sin \psi \tag{B7}$$

Denoting

$$c_2 = \frac{u}{c_1}\sin \psi \tag{B8}$$

the general solution of system (B7) can be written as

$$q_1(s) = G\sin(s+\beta) - c_2, \qquad q_2(s) = G\cos(s+\beta) \tag{B9}$$

where G and β are the gain and phase which are determined by the initial conditions. q_1 and q_2 can be obtained as functions of t by using the fact that $\cos i = \sqrt{1-q_1^2-q_2^2}$, and therefore

$$\frac{ds}{c_1\sqrt{1-q_1^2-q_2^2}} = dt \tag{B10}$$

Substituting for q_1 and q_2 from (B9),

$$\frac{ds}{c_1\sqrt{1-G^2-c_2^2+2c_2 G\sin(s+\beta)}} = dt \tag{B11}$$

Integrating both sides of (B11) in closed form is possible with the aid of elliptic integrals of the first kind. This integration will yield a relationship between s and t. Further details can be found in Kinoshita [7]. An additional simplification of (B11) is possible if we use the small inclination approximation, $\cos i \approx 1$. In this case, $s \approx c_1 t$, and

$$q_1(t) \approx G\sin(c_1 t + \beta) - c_2 \qquad q_2(t) \approx G\cos(c_1 t + \beta) \tag{B12}$$

The amplitude and phase are given, respectively, by

$$G = \sqrt{\sin^2 i_0 + c_2^2 + 2c_2 \sin i_0 \cos \Omega_0} \tag{B13}$$

$$\beta = \tan^{-1}\frac{\sin i_0 \cos \Omega_0 + c_2}{\sin i_0 \sin \Omega_0} \tag{B14}$$

Acknowledgements

The author wishes to thank Michael Efroimsky of USNO for motivating the problem discussed in the paper and David Mishne and Alex Kogan of the Asher Space Research Institute for making valuable comments.

References

[1] Landis, G. A., "Space Power by Ground-Based Laser Illumination," *IEEE Aerospace and Electronics Systems Magazine*, Vol. 6, No. 6, 1991, pp. 3–7.

[2] Eutelsat Website, http://www.eutelsat.com/home/index.html [cited 7 July 2004].

[3] Turner, A., "Orbit Dynamics of Cost-Effective Spacecraft for Frequent Non-Intrusive Servicing," *Advances in the Astronautical Sciences*, Vol. 109, 2001, pp. 711–728.

[4] Bretagnon, P., Fienga, A., and Simon, J.-L., "Expressions for the Precession Consistent with the IAU 2000A Model," *Astronomy and Astrophysics*, Vol. 400, 2003, pp. 785–790.

[5] Soop, E. M., *Handbook of Geostationary Orbits*, Kluwer Academic, Boston, 1994, Chap. 2, pp. 25–30.

[6] Goldreich, P., "Inclination of Satellite Orbits about an Oblate Precessing Planet," *The Astronomical Journal*, Vol. 70, No. 1, 1965, pp. 5–9.

[7] Kinoshita, H., "Motion of the Orbital Plane of a Satellite due to a Secular Change of the Obliquity of its Mother Planet," *Celestial Mechanics and Dynamical Astronomy*, Vol. 57, 1993, pp. 359–368.

[8] Efroimsky, M., and Goldreich, P., "Gauge Freedom in the N-body Problem of Celestial Mechanics," *Astronomy & Astrophysics*, Vol. 415, 2004, pp. 1187–1199.

[9] Chao, C. C., "Mathematical Derivations of the 'e-i' and Halo GEO Collocation Methods," *Advances in the Astronautical Sciences*, Vol. 109, No. 1, 2002, pp. 239–254.

[10] Vallado, D. A., *Fundamentals of Astrodynamics and Applications*, 2nd ed., Kluwer Academic, Boston, 2001, Chap. 8, pp. 518–521.

[11] Kechichian, J. A., "Optimal Steering for North-South Stationkeeping of Geostationary Spacecraft," *Journal of Guidance, Control, and Dynamics*, Vol. 20, No. 3, 1997, pp. 435–444.

[12] Battin, R. H., *An Introduction to the Mathematics and Methods of Astrodynamics*, AIAA, Reston, VA, 1999, Chap. 10, pp. 471–508.

[13] Bate, R. R., Mueller, D. D., and White, J. E., *Fundamentals of Astrodynamics*, Dover, New York, 1971, Chap. 2, pp. 71–83.

[14] Euler, L., *Opera Mechanica et Astronomica*, Birkhauser–Verlag, Switzerland, 1999, Chap. 2, pp. 45–62.

[15] Lagrange, J. L., "Sur la Théorie Générale de la Variation des Constants Arbitraries dans tous les Problèmes de la Méchanique," *Lu*, Vol. le 13 mars 1809 à l'Institut de France, 1809.

[16] Efroimsky, M., "Equations for the Orbital Elements. Hidden Symmetry," Preprint No. 1844 of the Institute of Mathematics and its Applications, University of Minnesota, available at http://www.i-ma.umn.edu/preprints/feb02/1844.pdf, 2002.

[17] Brouwer, D., and Clemence, G. M., *Methods of Celestial Mechanics*, Academic Press, New York, 1961, Chap. 5, pp. 452–503.

[18] King-Hele, D. G., "The Effect of the Earth's Oblateness on the Orbit of a Near Satellite," *Proceedings of the Royal Society of London, Series A: Mathematical and Physical Sciences*, Vol. 247, No. 1248, 1958, pp. 49–72.

[19] Newman, W., and Efroimsky, M., "The Method of Variation of Constants and Multiple Time Scales in Orbital Mechanics," *Chaos*, Vol. 13, 2003, pp. 476–485.

[20] Efroimsky, M., and Goldreich, P., "Gauge Symmetry of the N-body Problem in the Hamilton-Jacobi Approach," *Journal of Mathematical*

Physics, Vol. 44, 2003, pp. 5958–5977.
[21] Goldstein, H., Poole, C., and Safko, J., *Classical Mechanics*, Addison Wesley, New York, 2002, Chap. 8, pp. 334–339.
[22] Kamel, A., and Tibbitts, R., "Some Useful Results on Initial Node Location for Near-Equatorial Circular Satellite Orbits," *Celestial Mechanics*, Vol. 8, 1973, pp. 45–73.
[23] Palmer, P. L., and Hashida, Y., "Epicyclic Motion of Satellites About an Oblate Planet," *Journal of Guidance, Control, and Dynamics*, Vol. 24, No. 3, 2001, pp. 586–596.
[24] Coffey, S. L., and Deprit, E., "Frozen Orbits for Satellites Close to an Earth-Like Planet," *Celestial Mechanics and Dynamical Astronomy*, Vol. 59, No. 9, 1994, pp. 37–72.
[25] Khalil, H. K., *Nonlinear Systems*, Prentice–Hall, Upper Saddle River, NJ, 1996, Chap. 4, pp. 167–169.